

Sussex Research

RAD6-RAD18-RAD5-pathway-dependent tolerance to chronic low-dose ultraviolet light

T Hishida, Y Kubota, Antony Carr, H Iwasaki

Publication date

01-01-2009

Licence

This work is made available under the **Copyright not evaluated** licence and should only be used in accordance with that licence. For more information on the specific terms, consult the repository record for this item.

Citation for this work (American Psychological Association 7th edition)

Hishida, T., Kubota, Y., Carr, A., & Iwasaki, H. (2009). *RAD6-RAD18-RAD5-pathway-dependent tolerance to chronic low-dose ultraviolet light* (Version 1). University of Sussex.
<https://hdl.handle.net/10779/uos.23313566.v1>

Published in

Nature

Copyright and reuse:

This work was downloaded from Sussex Research Open (SRO). This document is made available in line with publisher policy and may differ from the published version. Please cite the published version where possible. Copyright and all moral rights to the version of the paper presented here belong to the individual author(s) and/or other copyright owners unless otherwise stated. For more information on this work, SRO or to report an issue, you can contact the repository administrators at sro@sussex.ac.uk. Discover more of the University's research at <https://sussex.figshare.com/>

***RAD6-RAD18-RAD5* pathway-dependent tolerance to chronic low-dose UV light**

Takashi Hishida¹, Yoshino Kubota¹, Tomoko Ohya¹, Antony M. Carr² & Hiroshi Iwasaki³

¹*Research Institute for Microbial Diseases, Osaka University, 3-1 Yamadaoka, Suita, Osaka 565-0871, Japan,*

²*MRC Genome Damage and Stability Centre, University of Sussex, Brighton, BN1 9RQ, UK*

³*International Graduate School of Arts and Sciences, Yokohama City University, Yokohama, Kanagawa 230-0045, Japan.*

In nature, organisms are exposed to chronic low-dose UV (CLUV) as opposed to the acute high doses common to laboratory experiments. Analysis of the cellular response to acute high-dose exposure has delineated the importance of direct DNA repair by the nucleotide excision repair pathway and for checkpoint-induced cell cycle arrest in promoting cell survival. Here we examine the response of yeast cells to CLUV and identify a key role for the *RAD6-RAD18-RAD5* error-free postreplication repair (*RAD6* error-free PRR) pathway in promoting cell growth and survival. We show that loss of the *RAD6* error-free PRR pathway results in DNA damage checkpoint-induced G₂ arrest in CLUV-exposed cells, whereas wild type and nucleotide excision repair (NER) deficient cells are largely unaffected. Cell cycle arrest in the absence of the *RAD6* error-free PRR pathway was not caused by a repair defect or by the accumulation of UV-induced photoproducts. Notably, we observed increased RPA- and Rad52-YFP foci in the CLUV-exposed *rad18*Δ cells and demonstrated that Rad52-mediated homologous recombination is required for the viability of the *rad18*Δ cells following release from CLUV-induced G₂ arrest. These and other data presented suggest that, in response to environmental levels of UV exposure, the *RAD6* error-free PRR pathway promotes replication of damaged templates without the generation of extensive single-stranded DNA regions. Thus, the error-free PRR pathway is specifically important during chronic low-dose UV exposure to prevent counter-productive DNA checkpoint activation and allow cells to proliferate normally.

The importance of DNA repair and damage tolerance for sunlight-induced DNA damage is evident from the highly elevated skin cancer incidence in patients with the genetic disease Xeroderma pigmentosum (XP)¹ which is caused by mutation of genes responsible for NER or damage bypass by error-prone DNA polymerases. Four highly conserved DNA damage response mechanisms make major contributions to the UV

response: NER, *RAD6* damage tolerance, homologous recombination (HR), and the DNA damage checkpoint^{2,3}.

In previous studies of the cellular UV response, high-dose UV (*i.e.*, 1 to 500 J/m²) was delivered within a relatively short time. However, such acute conditions are rare in environmental situations, where organisms are typically exposed continuously or intermittently to very low dose UV for extended periods. Here, we have explored the biological effects of continuous irradiation by low-dose UV, utilizing budding yeast as a model organism. On a sunny day, sunlight at the earth's surface equates to a dose-rate of ~0.1 J/m² per min from a 254 nm UV light^{4,5}. Therefore, we established “chronic low dose UV” (CLUV)-irradiation conditions by exposing cells to 0.18 J/m² per min UV (254 nm peak wavelength) using commercial germicidal lamps.

To examine cell growth, early logarithmic cells (liquid culture; 30°C) were exposed to CLUV and samples were taken every 3 h to determine plating efficiency (Fig. 1a). CLUV had no significant effect on growth of either wild-type (WT), HR-deficient (*rad52Δ*), checkpoint-deficient (*mec1Δ*) or, surprisingly, NER-deficient (*rad14Δ*) cultures. In contrast, a damage tolerance pathway-deficient strain (*rad18Δ*) did not increase in cell number and gradually lost viability. Similar results were observed in spot assays that examine effects of a longer period of CLUV exposure (Fig. 1b). We confirmed that *rad14Δ* cells are hypersensitive to acute UV irradiation (6 J/m²) and that *rad18Δ* cells are only moderately sensitive (Fig. 1b, right panel).

UV generates multiple DNA lesions, including cyclobutane pyrimidine dimers (CPD) and 6-4 photoproducts^{6,7}. To establish if *rad18Δ* CLUV hypersensitivity results from a higher load of DNA lesions, we used an immunoblot assay⁸ to quantify CPDs in CLUV-exposed cells. In WT and *rad18Δ* cells, CPDs accumulated to relatively low

levels during 9h of CLUV exposure (Fig. 1c). In NER-deficient (*rad14Δ*) cells, the CPD concentration increased to high levels. The total dose delivered by CLUV during 9 h corresponds 97 J/m², but WT and *rad18* cells accumulated damage equivalent to 2.3 J/m² (delivered in 5 sec, see Supplemental Fig.1), confirming that WT and *rad18Δ* cells are NER-proficient. Thus, the *RAD6-RAD18* pathway plays an essential role in the CLUV response even when the NER is actively eliminating UV-induced lesions.

The *RAD6-RAD18* damage tolerance consists of two mechanisms that allow lesion bypass by replication without lesion removal and is highly conserved in yeast and humans (Supplemental Table 1)⁹⁻¹¹. The first, translesion DNA synthesis (TLS) requires Rad18-dependent PCNA-K164 monoubiquitination and involves error-prone DNA polymerases^{12,13}. The second is error-free PRR, coordinated by Rad18 and Rad5-dependent PCNA-K164 polyubiquitination, and likely acts via transient template strand switching^{12,14}. Consistently, a *pol30-K164R* mutant (lacking the PCNA ubiquitin attachment site) was sensitive to CLUV exposure (Fig. 1d). A TLS-deficient strain (*tlsΔ*, a *rad30Δ rev3Δ rev1Δ* triple mutant) did not show detectable CLUV sensitivity, whereas a *rad5Δ* mutant showed CLUV hypersensitivity equivalent to *rad18Δ* and *rad6Δ* mutants (Fig. 1d), indicating the importance of error-free PRR to the CLUV response.

The Rad5 protein has a RING (E3 ligase) domain and a SWI2/SNF2 helicase domain with *in vitro* activity specific for fork structures. In addition to mediating the polyubiquitination of PCNA, Rad5 is shown to promote template switching through combined helicase and DNA annealing activities¹⁵. An ATPase-deficient *rad5-K538A* mutant showed CLUV hypersensitivity similar to the *rad5Δ* mutant (Fig. 1d), suggesting that Rad5-mediated template switching is required for tolerance to CLUV

exposure. Previous studies have shown that both *rad5Δ* and *pol30-K164R* are slightly less sensitive to acute UV than the *rad18Δ* strain¹². The same behavior was also observed in the CLUV sensitivity when cells were exposed to much less UV dose (<0.1 J/m²/min), consistent with the above idea that Rad5-dependent sub-pathway are responsible for CLUV tolerance (Supplementary Fig. 2).

To analyze the role of PRR in CLUV tolerance, asynchronous WT, *rad18Δ* and *rad5Δ* cultures were treated with CLUV for 6h and assayed by FACS. Cell cycle progression of WT cells was not significantly affected by CLUV exposure. However, the majority of *rad18Δ* and *rad5Δ* cells arrested with 2C DNA content (Fig. 2a). $>70\%$ arrested as large-budded cells with one nucleus at the bud neck and a short mitotic spindle (Fig. 2b, c). Cdc45 and MCM7 showed significantly reduced chromatin association in CLUV exposed *rad18Δ* compared to WT cells (Supplementary Fig. 3). These replication proteins only bind chromatin during S and G₁-S phase respectively, but not during G₂ phase^{16,17}. Thus, *RAD6* error-free PRR deficient cells are arrested in G₂ phase under the CLUV irradiation.

Next, cells were synchronized cells in G₁ and released into CLUV exposure conditions. The majority of WT, *rad18Δ* and *rad5Δ* cells entered and completed S phase within 60 min. However, while WT cells continued through G₂/M, *rad18Δ* and *rad5Δ* cells arrested with 2C DNA content before the first mitosis (Fig. 2d). Because *rad18Δ* and *rad5Δ* cells remain viable and resume growth after release from CLUV exposure (Fig. 1a and Supplementary Fig. 4a), we analysed *rad18Δ mec1Δ* and *rad5Δ mec1Δ* double mutants to establish if G₂ arrest contributed to viability. CLUV-exposed *rad18Δ mec1Δ* and *rad5Δ mec1Δ* cells did not arrest after release from G₁ into CLUV (Fig. 3a, b and Supplementary Fig. 4b) and failed to form colonies (Fig. 3c and Supplementary

Fig. 4a). To confirm that viability required G₂ arrest, the double mutant and the appropriate controls were arrested in G₂ with nocodazole during CLUV exposure (Fig. 3d). The majority of *rad18Δ mec1Δ* cells remained viable, indicating a critical role for G₂ arrest.

We also tested various checkpoint mutants¹⁸. Neither *tell1Δ*, *mrc1Δ* or *chk1Δ* significantly affected viability of CLUV-exposed *rad18Δ* cells (Fig. 3c). In contrast, *rad18Δ rad53Δ* and *rad18Δ rad9Δ*, like *rad18Δ mec1Δ* reduced viability (Fig. 3c), suggesting that the Mec1-Rad9-Rad53-dependent DNA damage checkpoint is activated. The same behavior was also observed in *rad5Δ* derivatives (Supplementary Fig. 4a). We thus analyzed Rad53 phosphorylation (Fig. 3e). Hyperphosphorylated Rad53 was not detected in WT cells following 6 h of CLUV exposure. In *rad18Δ* mutants, hyperphosphorylated Rad53 was evident after 2 h of CLUV exposure and accumulated with exposure time. This hyperphosphorylation is Mec1- and Rad9-dependent (Fig. 3e). Ddc2 is the Mec1 binding partner that recognizes RPA-coated single-stranded DNA (ssDNA)¹⁹. We also observed a significant increase in Ddc2 foci following CLUV exposure in *rad18Δ* and *rad5Δ* cells (Supplementary Fig. 5), a recognized hallmark of checkpoint activation²⁰. Thus, our results clearly indicate that the Mec1-Rad9-Rad53-dependent DNA damage checkpoint is activated by CLUV exposure in cells defective for the *RAD6* error-free PRR pathway. Rad9 functions predominantly in the G₁/S and G₂/M checkpoints, playing only a minor role in the DNA replication checkpoint during S phase²¹. This, and the lack of increased sensitivity upon *MRC1* deletion, supports an interpretation of G₂ checkpoint arrest during CLUV exposure.

Acute high-dose UV-treatments result in the accumulation of ssDNA gaps when cells initiate DNA replication²²⁻²⁴. We thus examined the subcellular localization of

RPA-YFP during CLUV exposure of *rad18Δ* cells. Few RPA-YFP foci were observed in untreated WT, *rad18Δ* or *rad5Δ* cells. After 3 h of CLUV exposure, RPA-YFP foci were observed in ~80% of *rad18Δ* and *rad5Δ* cells but only ~10% of WT cells (Fig. 4a). Following release from G₁ into CLUV conditions, *rad18Δ*, but not WT, cells rapidly accumulated RPA-YFP foci and arrested with a budded morphology (Fig. 4b). These results suggest that ssDNA gaps accumulate in CLUV-exposed *rad18Δ* cells that likely result in G₂ arrest.

RPA-coated ssDNA gaps at stalled replication forks are both competent for and required for HR^{25,26}. Therefore, we analyzed subcellular localizations of the key HR protein Rad52. Rad52 foci were significantly increased in CLUV-exposed cells *rad18Δ* and *rad5Δ* mutants compared to WT (Supplementary Fig. 6), implying activation of HR. Deletion of *RAD52* caused viability loss in CLUV-exposed *rad18Δ* cells, although *rad52Δ rad18Δ* double mutant cells were competent for CLUV-induced G₂ arrest (Fig. 4c, d and Supplementary Fig. 7). Interestingly, unlike *rad18Δ* single mutant cells, *rad18Δ rad52Δ* double mutant cells could not resume cell cycle progression following cessation of CLUV treatment (Fig. 4e and Supplementary Fig. 8). These results demonstrate that *rad18Δ rad52Δ* cells are not checkpoint-defective, but are unable to recover from CLUV-induced G₂ arrest. Thus, Rad52 play a critical role in CLUV tolerance that is required for reversible G₂ arrest in the absence of *RAD6* error-free PRR.

We show that cells defective in the error-free Rad6-Rad18-Rad5-dependent PRR pathway complete bulk DNA replication during CLUV exposure, but generate ssDNA lesions that cause G₂ arrest and require time for repair by HR proteins (Fig. 4f). Recent evidence suggests that replication forks blocked by DNA lesions can be rescued by

downstream re-priming of both the leading and lagging strands in both *E. coli* and *S. cerevisiae*^{24,27}. This could result in replication completion, but at the expense of ssDNA gaps spanning the fork-blocking lesion. The observation that CLUV exposure lead to an increased number of RPA and Ddc2 foci and checkpoint activation in cells defective in error-free PRR supports this model (Fig. 4f).

In summary, in response to continuous exposure to extremely low-dose UV, the DNA damage checkpoint is not activated in WT cells because the *RAD6-RAD18-RAD5* dependent error-free PRR pathway plays a critical role by preventing the generation of excessive ssDNA when replication forks arrest, thus suppressing counter-productive checkpoint activation. While the DNA damage checkpoints are critical for genome stability because it allows time for accurate DNA repair and the induction of apoptosis in higher eukaryotes, such a strategy is likely counter-productive at extremely low levels of DNA damage. Our study provides the first evidence error-free PRR prevents such activation at low doses of UV exposure in the model organism *S. cerevisiae*. Further studies on the biological implications of *RAD6* pathway during chronic low dose damage exposure in other species will be of great interest.

Methods Summary

Standard methods were used to construct strains carrying deletion alleles or epitope-tagged proteins. To synchronize cells in G₁ and G₂, α factor (10 μ g/ml, Sigma) and nocodazole (15 μ g/ml, Sigma) was added to cells in mid-log phase ($\sim 5 \times 10^6$ cells/ml), respectively, and followed by incubation for 2 h at 30°C. For CLUV irradiation, cell cultures were incubated with horizontal shaking at 30°C under continuous exposure to 0.18 J/m²/min. Dot blot analysis for genomic DNA was performed as described

previously⁸. DNA with CPDs was detected using monoclonal antibody against thymidine dimer (TDM2). Flow cytometry, western blotting and microscopic analysis were performed as described previously²⁸. See Supplemental information for details.

References

- 1 E. C. Friedberg, *Nat Rev Cancer* **1**, 22-33 (2001).
- 2 S. Prakash, P. Sung, and L. Prakash, *Annu Rev Genet* **27**, 33-70 (1993).
- 3 J. C. Game, *Mutat Res* **451**, 277-293 (2000).
- 4 W. Harm, *Radiat Res* **40**, 63-69 (1969).
- 5 A. J. Callegari and T. J. Kelly, *Proc Natl Acad Sci U S A* **103**, 15877-15882 (2006).
- 6 J. H. Hoeijmakers, *Nature* **411**, 366-374 (2001).
- 7 E. C. Friedberg, A. Aguilera, M. Gellert et al., *DNA Repair (Amst)* **5**, 986-996 (2006).
- 8 S. Giavara, E. Kosmidou, M. P. Hande et al., *Curr Biol* **15**, 68-72 (2005).
- 9 S. Prakash, R. E. Johnson, and L. Prakash, *Annu Rev Biochem* **74**, 317-353 (2005).
- 10 H. D. Ulrich, *ChemBiochem* **6**, 1735-1743 (2005).
- 11 P. L. Andersen, F. Xu, and W. Xiao, *Cell Res* **18**, 162-173 (2008).
- 12 C. Hoege, B. Pfander, G. L. Moldovan et al., *Nature* **419**, 135-141 (2002).
- 13 P. Stelter and H. D. Ulrich, *Nature* **425**, 188-191 (2003).
- 14 H. Zhang and C. W. Lawrence, *Proc Natl Acad Sci U S A* **102**, 15954-15959 (2005).
- 15 A. Blastyak, L. Pinter, I. Unk et al., *Mol Cell* **28**, 167-175 (2007).
- 16 C. Liang and B. Stillman, *Genes Dev* **11**, 3375-3386 (1997).
- 17 L. Zou and B. Stillman, *Science* **280**, 593-596 (1998).
- 18 M. Foiani, A. Pelliccioli, M. Lopes et al., *Mutat Res* **451**, 187-196 (2000).
- 19 L. Zou and S. J. Elledge, *Science* **300**, 1542-1548 (2003).
- 20 V. Paciotti, M. Clerici, G. Lucchini et al., *Genes Dev* **14**, 2046-2059 (2000).
- 21 Z. Sun, J. Hsiao, D. S. Fay et al., *Science* **281**, 272-274 (1998).
- 22 W. D. Rupp and P. Howard-Flanders, *J Mol Biol* **31**, 291-304 (1968).
- 23 L. Prakash, *Mol Gen Genet* **184**, 471-478 (1981).
- 24 M. Lopes, M. Foiani, and J. M. Sogo, *Mol Cell* **21**, 15-27 (2006).
- 25 E. Fanning, V. Klimovich, and A. R. Nager, *Nucleic Acids Res* **34**, 4126-4137 (2006).
- 26 V. Gangavarapu, S. Prakash, and L. Prakash, *Mol Cell Biol* **27**, 7758-7764 (2007).
- 27 R. C. Heller and K. J. Mariani, *Nat Rev Mol Cell Biol* **7**, 932-943 (2006).
- 28 T. Hishida, T. Ohno, H. Iwasaki et al., *Embo J* **21**, 2019-2029 (2002).

Acknowledgements We thank R. Rothstein and H. Araki for strains and T. Matsunaga for anti-TDM2 antibody. This work was supported by a Sumitomo foundation and a Grant-in-Aid for Scientific Research from the Ministry of Education, Culture, Sports, Science and Technology of Japan.

Author Contributions T.H. designed the study. T.H., Y.K. and T.O. performed the experiments. H.I. coordinated the study. T.H., H.I. and A.M.C. analysed data and wrote the paper.

Author Information Correspondence and requests for materials should be addressed to T.H. (e-mail: hishida@biken.osaka-u.ac.jp)

Figure Legends

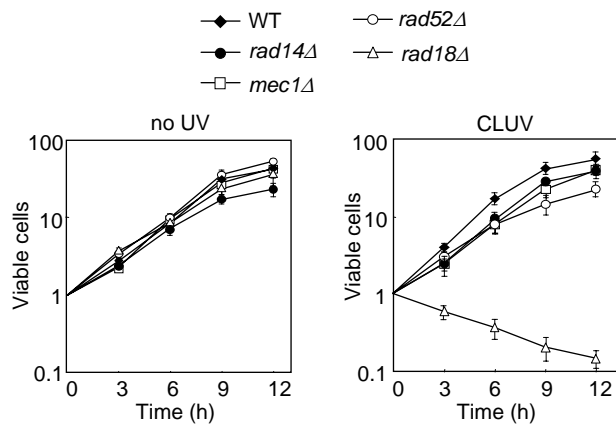
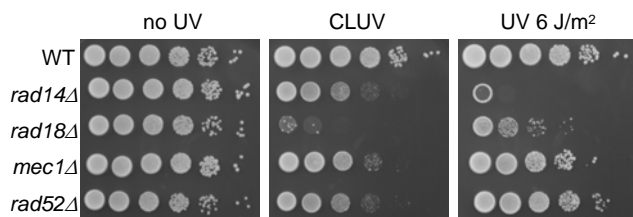
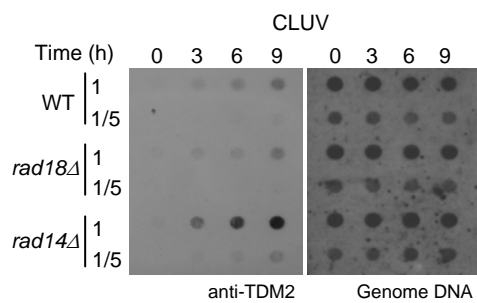
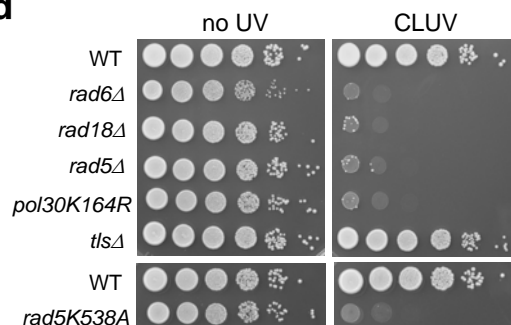
Figure 1 Role of the *RAD6* pathway in tolerance to CLUV exposure. **a**, The plating efficiency for WT, *rad14Δ*, *mec1Δ*, *rad52Δ* and *rad18Δ* strains under exposure to CLUV irradiation. Asynchronized log-phase cells were grown in rich media under CLUV irradiation and samples were taken every 3h to determine plating efficiency. Viable cells are represented as relative colony forming units (Time 0 =1), which were obtained from at least three independent experiments. The error bars indicate the standard deviations. The *mec1Δ* strain contains a deletion of *SML1*, which suppress the lethality without suppressing its checkpoint defect. The *sm1Δ* single mutation did not affect the growth under CLUV irradiation (data not shown). **b**, Ten-fold serial dilutions of stationary-phase cells were spotted onto plates. DNA damage was induced by acute UV irradiation (6 J/m²; right panel) or CLUV exposure for 2 days (middle panel). **c**, Dot blot analysis of DNA extracted from **a** using anti-CPD antibody. **d**, CLUV sensitivity of *RAD6* pathway mutants. Cells were exposed to CLUV as in **b**.

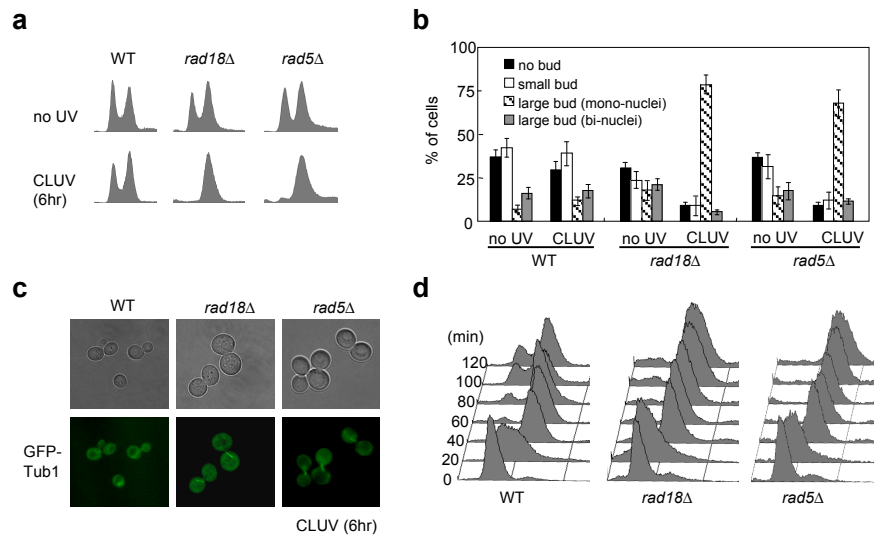
Figure 2 A deficiency in Rad18 causes G₂ arrest in response to CLUV exposure. **a**, Flow cytometry of WT, *rad18Δ* and *rad5Δ* cells exposed to CLUV for 6 h. **b**, Cells from **a** were stained with DAPI to evaluate nuclear and cellular morphology. **c**, Cells expressing GFP-TUB1 were treated as in **a** and spindles were visualized by fluorescence microscopy. **d**, Flow cytometry of synchronized WT, *rad18Δ* and *rad5Δ* cells under CLUV irradiation. Cells were synchronized with α -factor, transferred to fresh medium, and exposed to CLUV for the indicated time.

Figure 3 DNA damage checkpoint activation in CLUV-exposed *rad18Δ* cells. **a**, WT, *rad18Δ*, *mec1Δ* and *mec1Δ rad18Δ* cells were synchronized at G₁ with α -factor, transferred to fresh medium, and exposed to CLUV for the indicated time. **b**, The strains from **a** were exposed to CLUV for 6 h, harvested and stained with DAPI. **c**, Cells were grown and treated as in Fig. 1**a**. **d**, Nocodazole rescues CLUV-induced *mec1 rad18* lethality. Cells were synchronized in G₂/M with nocodazole, exposed to CLUV for the indicated time in the presence or absence of nocodazole and plating efficiency was determined. **e**, CLUV-induced Rad53 phosphorylation in cells expressing *RAD53-9Myc*. Protein extracts from cells treated as in **a** were prepared and analyzed by 5% SDS-PAGE followed by Western blotting using anti-Myc (9E10) antibody. α -Tubulin was used as a loading control.

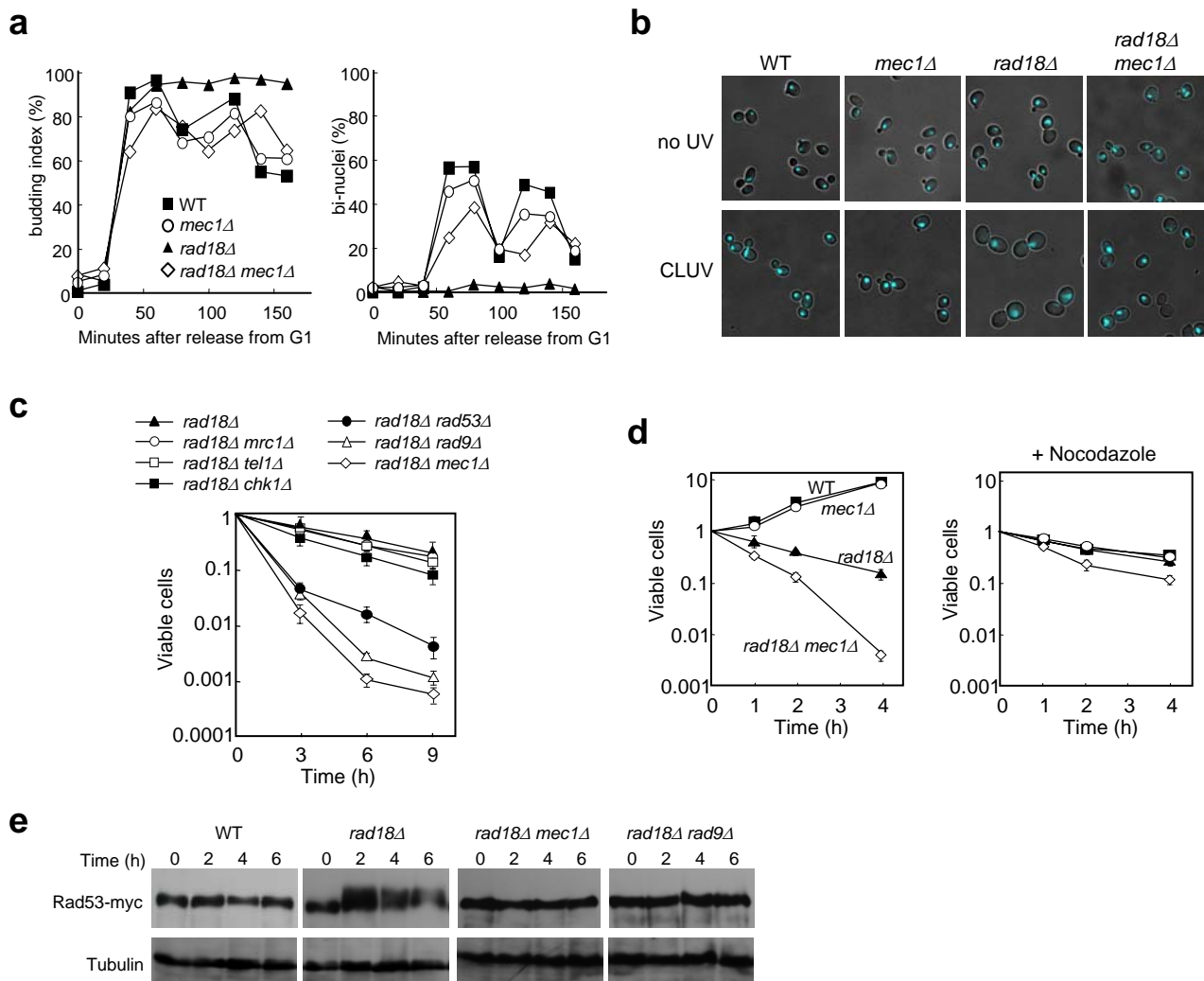
Figure 4 CLUV-induced DNA damage in *rad18Δ* cells. **a**, CLUV induces RPA foci in *rad18Δ* cells. Asynchronous cultures of WT and *rad18Δ* cells were treated with CLUV for 3 h and examined by fluorescence microscopy. **b**, Cell cycle distribution of CLUV-induced RPA foci. Synchronized cells were released into CLUV exposure conditions and analyzed microscopically for the presence of budded (WT, filled circle; *rad18Δ*, filled square) and RPA-foci containing (WT, open circle; *rad18Δ*, open square) cells. **c**, Plating efficiency of *rad52Δ rad18Δ* cells exposed to CLUV. Cells were grown and treated as in Fig. 1**a**. **d**, Cell cycle progression of *rad52Δ rad18Δ* cells. The experiments were performed as described in Fig. 3**a**. **e**, Flow cytometry of *rad18Δ* and *rad18Δ rad52Δ* cells after release from CLUV exposure for 3 h. Aliquots were taken at the indicated time after terminating CLUV. **f**, A model for the CLUV damage tolerance in yeast. (i), Under CLUV conditions, most UV lesions are quickly repaired by NER,

but lesions remaining at the onset of S phase blocks replication fork progression. (ii), The *RAD6-18-5* error-free PRR pathway promotes replication across the damaged template, likely by using the newly synthesized sister chromatid as a template. This enables cells to complete replication without ssDNA gap accumulation. (iii). This contributes to suppression of checkpoint activation and allows cells to continue growth under CLUV irradiation. (iv), In PRR deficient cells, DNA replication of the damaged template is still completed by other replication-bypass mechanisms, possibly involving repriming downstream of the damage. (v), This generates ssDNA gaps that activate the DNA damage checkpoint and are subsequently be repaired by *RAD52*-dependent mechanisms during the CLUV-induced cell cycle delay. Triangles represent the UV lesions.

a**b****c****d**



Hishida et al._Fig. 2



Hishida et al._Fig. 3

